Inorg. Chem. **2002**, *41*, 1365–1371

Ruthenium Complexes of Analogues of the Antitumor Antibiotic Streptonigrin

Pia I. Anderberg, Margaret M. Harding,* Ian J. Luck, and Peter Turner

School of Chemistry, University of Sydney, N.S.W. 2006, Australia

Received August 14, 2001

The complexes Ru(**L1**–CH_3)$(CO)_3Cl$, Ru**L2**$(CO)_2Cl_2$, and Ru**L3**$(CO)_2Cl_2$ (**L1**= 6-methoxy-5,8-quinolinedione, **L2** = 7-amino-6-methoxy-5,8-quinolinedione, **L3** = 6,6′-dimethoxycarbonyl-2,2′-bipyridine) were prepared by reaction of **L1**–**L3** with the tricarbonyldichlororuthenium(II) dimer. **L1**–**L3** act as bidentates through the ortho oxygen atoms, the pyridyl nitrogen and the adjacent quinone oxygen, and the bipyridyl nitrogens, respectively. Ru**L3**$(CO)_2Cl_2$ is characterized by X-ray crystallography. ^{15}N NMR correlation spectra give upfield shifts of around 60 ppm for the pyridyl nitrogens that are coordinated to the metal, while ^{13}C NMR correlation spectra give a downfield shift of 10 ppm for the quinone carbonyl group that is coordinated to the metal. The electrochemistry of Ru**L2**$(CO)_2Cl_2$ is examined, and the implications for the formation of metal complexes of the antitumor antibiotic streptonigrin, which cleaves DNA in the presence of metal ions, are discussed.

Introduction

Streptonigrin is a functionalized 7-aminoquinoline-5,8-dione that is highly active against a variety of human cancers.[1−4] Extensive in vitro studies suggest that DNA is the principle cellular target responsible for anticancer activity and that this activity is directly related to streptonigrin-mediated DNA strand scission.[5−8] However, in contrast to other well-characterized aminoquinone antitumor antibiotics (eg., daunomycin, mitomycin), the mechanism of DNA strand cleavage is unique in its reliance on metal ions.[9−11] While the exact role of transition metal ions in the mechanism of action of streptonigrin is still not fully understood,[12] it has been proposed that metals function as delivery agents of streptonigrin or reduced streptonigrin to DNA via an electrostatic interaction[12−14] and/or that they catalyze the production of the DNA-damaging species.[8,15,16]

Because of the important role of transition metal ions in the mechanism of antitumor action of streptonigrin, the effects of a number of metal ions on the properties of streptonigrin have been reported. A range of divalent transition metal ions enhances the biological activity of streptonigrin, and metal complexes of streptonigrin with zinc(II),[13,17−19] copper(II),[11,17,19] cadmium(II),[18] cobalt(II),[11,20] iron(II),[11,20] manganese(II),[19] palladium(II),[21] ytterbium(III),[20] and gold(III)[22] have been reported.

^1H NMR studies reveal that the interaction of zinc(II) with streptonigrin results in the formation of multiple complexes whose structures and stabilities are solvent-dependent.[13] The carbonyl groups flanking the bipyridyl assist in stabilization of the complexes, and under biologically relevant conditions, streptonigrin forms a 1:1 bipyridyl complex in the presence of a large excess of zinc(II) (Figure 1).[13] ^1H NMR studies

* Corresponding author. E-mail: harding@chem.usyd.edu.au. Fax: +612-9351-6650.

(1) Wilson, W. L.; Labra, C.; Barrist, E. *Antibiot. Chemother.* **1961**, *11*, 147.
(2) Sullivan, R. D.; Miller, E.; Zurek, W. Z.; Rodriguez, F. R. *Cancer Chemother. Rep.* **1963**, *33*, 27.
(3) Hackerthal, C. A.; Golbey, R. B. *Antibiot. Chemother.* **1961**, *11*, 178.
(4) Hajdu, J. *Metal. Ions Biol. Syst.* **1985**, *19*, 53.
(5) Gutteridge, J. M. *Biochem. Pharmacol.* **1984**, *33*, 3059.
(6) Cone, R.; Hasan, S. K.; Lown, J. W.; Morgan, A. R. *Can. J. Biochem.* **1976**, *54*, 219.
(7) White, J. R. *Biochem. Biophys. Res. Commun.* **1977**, *77*, 387.
(8) Hassett, D. J.; Britigan, B. E.; Svendsen, T.; Rosen, G. M.; Cohen, M. S. *J. Biol. Chem.* **1987**, *262*, 13404.
(9) Shaikh, I. A.; Johnson, F.; Grollman, A. P. *J. Med. Chem.* **1986**, *29*, 1329.
(10) Lown, J. W.; Sim, S. *Can. J. Biochem.* **1976**, *54*, 446.
(11) Lown, J. W.; Sim, S. K. *Can. J. Chem.* **1976**, *54*, 2563.
(12) Harding, M. M.; Long, G. V. *Curr. Med. Chem.* **1997**, *4*, 405.
(13) Long, G. V.; Harding, M. M. *J. Chem. Soc., Dalton Trans.* **1996**, 549.
(14) Soedjak, H. S.; Cano, R. E.; Tran, L.; Bales, B. L.; Hajdu, J. *Biochim. Biophys. Acta* **1997**, *1335*, 305.
(15) White, J. R. *Biochem. Biophys. Res. Commun.* **1977**, *77*, 387.
(16) Yeowell, H. N.; White, J. R. *Antimicrob. Agents Chemother.* **1982**, *22*, 961.
(17) Hajdu, J.; Armstrong, E. C. *J. Am. Chem. Soc.* **1981**, *103*, 232.
(18) Soedjak, H.; Hajdu, J.; Raffetto, J. D.; Cano, R.; Bales, B. L.; Prasad, L. S.; Kispert, L. D. *Biochim. Biophys. Acta* **1997**, *1335*, 73.
(19) Rao, K. V. *J. Pharm. Sci.* **1979**, *68*, 853.
(20) Wei, X.; Ming, L. *J. Chem. Soc., Dalton Trans.* **1998**, 2793.
(21) Fiallo, M. M. L.; Garnier-Suillerot, A. *Inorg. Chem.* **1990**, *29*, 893.
(22) Moustatih, A.; Garnier-Suillerot, A. *J. Med. Chem.* **1989**, *32*, 1426.

10.1021/ic010876m CCC: $22.00
Published on Web 02/21/2002

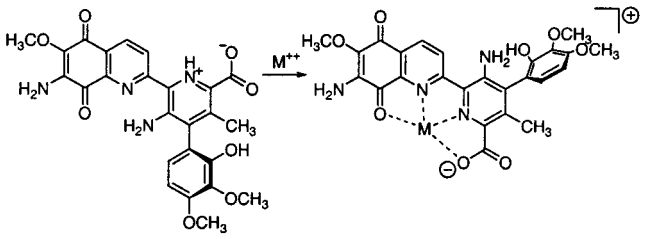

Figure 1. Proposed complex formed by streptonigrin and M(II) involving the carbonyl and carboxylate groups.

of the interaction of the paramagnetic ions iron(II), cobalt (II), and ytterbium(III) with streptonigrin are also consistent with formation of bipyridyl complexes.[20] However, there are no X-ray crystal structures of any metal complexes of streptonigrin, and the exact binding site(s) and coordination geometry of the metal center in metal complexes of streptonigrin, which would be useful in the design of metal complexes for drug testing,[12] are unknown.

Structure activity studies have examined the role of each of the four aromatic rings (A−D) of streptonigrin and the

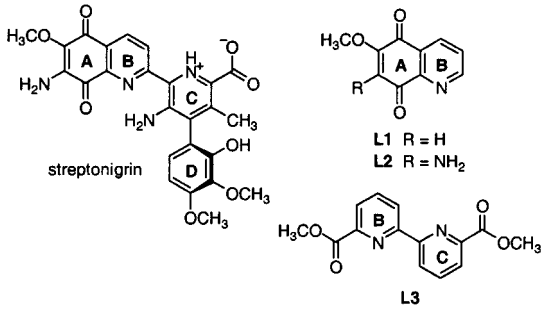

effects of the peripheral functional groups on biological activity. The presence of the A, B, and C rings, including the redox-active quinone in ring A, is essential.[4,12,23,24] The key metal binding groups, including the pyridyl nitrogens in rings B and C and the carboxylic acid group on ring C, are also essential for high activity.[25] In contrast, the role of ring D, which confers chirality on the drug,[26] is unclear. Analogues lacking this ring are more potent than streptonigrin or analogues containing only rings A and B.[24,27]

To increase the understanding of the role of metal ions in the activity of streptonigrin and to assist in the development of stable metal complexes of streptonigrin as potential anticancer agents,[12] we report the design and synthesis of ruthenium complexes of three analogues of streptonigrin, **L1**−**L3**. Ligands **L1** and **L2** are AB-ring analogues containing the redox active quinolinedione, and they differ from each other by the presence (**L2**) or absence (**L1**) of the amino group, an additional potential coordination site in these ligands. Ligand **L3** is a BC-ring analogue and contains the 2,2′-bipyridyl group with carbonyl groups at the 6,6′ positions; therefore, **L3** mimics the proposed metal binding site in streptonigrin[4,13,20] (Figure 1). Ruthenium(II) was chosen for this study because it forms kinetically inert complexes with nitrogen-donor ligands. This feature is in contrast with previous studies of streptonigrin and model ligands with labile metals including zinc(II), which precluded isolation and full structural characterization of the complexes by crystallographic analysis. In addition to standard characterization techniques, ^{15}N NMR spectroscopy was used as a chemical-shift probe to assign the site of complexation in solution. These studies, which included experiments to determine the electrochemical behavior of complex **2**, were carried out to further clarify the role of metal ions in the mechanism of action of streptonigrin and to assess the potential of ruthenium(II) in the development of a stable metal complex of streptonigrin.

Experimental Section

General. Ligands **L1** and **L2** were prepared by a modified literature procedure.[28] Ligands **L3** and 6,6′-dimethyl-2,2′-bipyridine (**L4**)[29] and dicarbonyl-(6,6′-dimethyl-2,2′-bipyridine)ruthenium(II) dichloride[30] (complex **4**) were prepared according to literature procedures. Tricarbonyldichlororuthenium(II) dimer was purchased from Aldrich and was used as received. Melting points were measured on a Reichardt hot stage and were not corrected. ^{1}H NMR spectra were recorded a Bruker AC200, AMX400, or AMX600 MHz spectrometer solvent-locked on deuterium and referenced to residual solvent peaks. Electron ionization mass spectra were recorded on a VG Autospec spectrometer at 70 eV. Electrospray (ES) mass spectra were recorded on a LCQ ion trap spectrometer using a capillary voltage of +10 V (positive ion). Values of *m*/*z* are expressed as percentages of the base-peak intensity in parentheses. Infrared spectra were recorded on a Perkin-Elmer 1600 FT-IR spectrometer. Microanalyses were performed by the microanalytical unit at the University of Otago, New Zealand.

Tricarbonyl-(6-quinolinide-5,8-dione)ruthenium(II) Chloride (1). Tricarbonyldichlororuthenium(II) dimer (68 mg, 132 μmol) was refluxed under nitrogen in THF (5 mL) for 18 h. Ligand **L1**, 6-methoxy-5,8-quinolinedione (50 mg, 264 μmol), in THF (7.5 mL) was added, and the solution was refluxed under nitrogen, in the dark, for 19 h. The resulting deep red-orange precipitate was isolated by filtration, washed with diethyl ether (2 mL), and dried to give [Ru(**L1**−CH_3)$(CO)_3$Cl] **(1)** (51 mg, 49%) with mp > 300 °C. Anal. Calcd for $C_{12}H_4ClNO_6Ru$: C, 36.5; H, 1.0; N, 3.5; Cl, 9.0. Found: C, 37.0; H, 0.9; N, 3.5; Cl, 9.0. IR (CH_2Cl_2) υ_{max}: 2140, 2084, 2058 (CO) cm^{-1}. ^{1}H NMR (200 MHz, acetone-d_6): δ 5.94 (1H, s, H 7), 8.00 (1H, dd, J = 5.6 Hz, J = 7.8 Hz, H3), 8.57 (1H, dd, J = 1.5 Hz, J = 7.7 Hz, H4), 9.22 (1H, dd, J = 1.5 Hz, J = 5.6 Hz, H2). ^{13}C NMR (150 MHz, acetone-d_6): δ 111.6 (C 7), 129.6 (C3), 139.1 (C 4), 157.8 (C2). ^{15}N NMR (40.5 MHz, acetone-d_6): δ 330 (N1). MS *m*/*z*: 395 (M^+, 5%), 367 (M − CO, 100), 339 (M − 2CO, 53), 311 (M − 3CO, 40).

Dicarbonyl-(7-amino-6-methoxy-5,8-quinolinedione)ruthenium(II) Dichloride (2). Ligand **L2**, 7-amino-6-methoxy-5,8-quinolinedione, (20 mg, 98 μmol) was treated with tricarbonyldichlororuthenium(II) dimer (25 mg, 49 μmol) according to the method used in the preparation of **1**. Degassed ether (3 mL) was

(23) Gould, S. J.; Weinreb, S. M. *Fortschr. Chem. Org. Naturst.* **1982**, *41*, 77.
(24) Boger, D. L.; Yasuda, M.; Mitscher, L. A.; Drake, S. D.; Kitos, P. A.; Thompson, S. C. *J. Med. Chem.* **1987**, *30*, 1918.
(25) Rao, K. V. *Cancer Chemother. Rep.* **1974**, *4*, 11.
(26) Tennant, S.; Rickards, R. W. *Tetrahedron* **1997**, *53*, 15101.
(27) Rao, K. V. *J. Heterocyclic Chem.* **1977**, *14*, 653.
(28) Liao, T. K.; Nyberg, W. H.; Cheng, C. C. *J. Heterocycl. Chem.* **1976**, *13*, 1063.
(29) Tiecco, M.; Testaferri, L.; Tingoli, M.; Chianelli, D.; Montanucci, M. *Synthesis* **1984**, *9*, 736.
(30) Homanen, P.; Haukka, M.; Pakkanen, T. A.; Pursianinen, J.; Laitinen, R. H. *Organometallics* **1996**, *15*, 4081.

added to the final solution to give a black solid, which was isolated under a stream of nitrogen by filtration, washed with diethyl ether (2 mL), and dried to give [Ru**L2**$(CO)_2Cl_2$] (**2**) (25 mg, 59%) with mp > 300 °C. IR (CH_2Cl_2) υ_{max}: 2075, 2011 (CO) cm^{-1}. ^1H NMR (200 MHz, acetone-d_6): δ 4.24 (3 H, s, OCH_3), 6.67 (2 H, s, NH_2), 8.23 (1 H, dd, $J = 5.3$ Hz, $J = 9.0$ Hz, H3), 8.61 (1 H, dd, $J = 1.1$ Hz, $J = 9.0$ Hz, H4), 9.28 (1 H, dd, $J = 1.1$ Hz, $J = 5.3$ Hz, H2). ^{13}C NMR (150 MHz, acetone-d_6): δ 62.5 (OCH_3), 131.4 (C4a), 134.0 (C3), 137.4 (C4), 140.2 (C 7), 142.1 (C6), 149.2 (C8a), 155.9 (C2), 176.2 (C5), 191.4 (C8), 196.7 (CO), 198.3 (CO). ^{15}N NMR (40.5 MHz, acetone-d_6): δ 258 (N1), 60 (NH_2). MS *m*/*z*: 434 (M^+, ^{104}Ru, 9), 431 (M^+, ^{102}Ru, 9), 403 (M − CO, 13), 375 (M − 2CO, 24), 204 (M − $(CO)_2Cl_2Ru$, 100). HRMS: calcd for $C_{12}H_8N_2O_5Cl_2{}^{104}Ru$, 433.8863; found, 433.8870.

Dicarbonyl-(6,6′-dimethoxycarbonyl-2,2′-bipyridine)ruthenium(II) Chloride (3). Ligand **L3**, 6,6′-dimethoxycarbonyl-2,2′-bipyridine, (42 mg, 154 μmol) was treated with tricarbonyldichlororuthenium(II) dimer (40 mg, 78 μmol) according to the method used in the preparation of **1**. The complex was washed with light petroleum followed by diethyl ether and was dried to give [Ru**L3**$(CO)_2Cl_2$] (**3**) as a tan solid (51 mg, 66%) with mp > 300 °C. Anal. Calcd for $C_{16}H_{12}Cl_2N_2O_6Ru$: C, 38.4; H, 2.4; N, 5.6. Found: C, 38.8; H, 2.3; N, 5.6. IR (CH_2Cl_2) υ_{max}: 1742 (CO_2CH_3), 2013 (CO), 2073 (CO) cm^{-1}. ^1H NMR (400 MHz, acetone-d_6): δ 3.96 (3 H, s, OCH_3), 4.16 (3 H, s, OCH_3), 8.12 (2 H, d, $J = 7.8$ Hz, H5), 8.48 (1 H, t, $J = 8.0$ Hz, H4), 8.56 (1 H, t, $J = 8.0$ Hz, H4′), 8.89 (2 H, app t, $J = 10.2$ Hz, H3). ^{13}C NMR (100 MHz, acetone-d_6): δ 53.1 (OCH_3), 54.3 (OCH_3), 126.3, 127.1, 127.9, 128.2, 141.6, 142.6, 154.5, 155.3, 158.6, 160.0, 164.8, 166.3, 192.3 (CO), 196.8 (CO). ^{15}N NMR (40.5 MHz, acetone-d_6): δ 231 (N1), 247 (N1′). ES *m*/*z*: 464.8 (M − Cl, 31), 436.8 (M − COCl, 100), 408.8 (M − $(CO)_2Cl$, 23). Crystals suitable for X-ray diffraction were obtained from a CH_2Cl_2 solution by slow evaporation of the solvent.

^{13}C and ^{15}N NMR Spectroscopy. ^{13}C NMR spectra (100.21 MHz) and ^{15}N NMR spectra (40.5 MHz) were recorded at 300 K on a Bruker DPX400 instrument with a tunable 5 mm multinuclear probe. Spectra were referenced to residual solvent (^{13}C) or neat external nitromethane (^{15}N, 379.5 ppm) signals. $^1H-^{13}C$ NMR correlation experiments were performed using standard manufacturer-supplied gs-HSQC and gs-HMBC pulse programs. The proton spectral window was sampled between 0 and 10.0 ppm in F2, and the F1 window was sampled from ~0 to 200 ppm. Typically, data was acquired with 2048 points in t_2, and the number of increments for time evolution was 512. The number of scans per increment was 32, and the delay between transients was 2 s. $^1H-^{15}N$ NMR correlation experiments were also performed using standard gs-HSQC and gs-HMBC pulse programs. The proton spectral window was sampled between 6 and 10.0 ppm in F2, and the F1 window was sampled over a sweep window of up to 200 ppm. HSQC experiments were optimized for N−H coupling of 90 Hz. Multiple bond-correlation experiments were optimized for long-range couplings of 2 Hz, with no decoupling applied during acquisition. Typically, data was acquired with 2048 points in t_2, and the number of increments for time evolution was varied from 100 to 512. The number of scans per increment varied from 48 to 600, and the delay between transients was 2 s. Total acquisition time ranged from 3 to 60 h. Data sets were zero-filled and Fourier transformed to give a final matrix of 2048 × 1024 points using sinebell weighting functions.

Cyclic Voltammetry Experiments. Cyclic voltammetry was conducted using a BAS-100 electrochemical analyzer employing a three-electrode system with 95−100% iR_u compensation in all solutions. The working electrode (WE) was a 0.8 mm-radius platinum (Pt) inlaid disk electrode (BAS). A platinum-wire counter electrode (CE) and a Ag/AgCl/KCl(sat) reference electrode (RE) were used in all experiments. The WE was polished regularly using a suspension of alumina (0.04 mm, Struers, FF Alumina) in Millipore water on a polishing cloth (Presi, Supra- Black).

All experiments were performed at 22 ± 1 °C. The concentration of the electroactive species was 1 mM, and the electrolyte was tetrabutylammonium perchlorate (TBAP) (0.1 M) in THF. Water was purified using a Millipore Alpha-Q system. THF was of analytical grade and was distilled from benzophenone and sodium wire prior to use. All samples were purged with argon for at least 20 min prior to use and were kept under a continuous flow of argon during the course of the experiments. The argon was purified to remove all oxygen and water. The purification system consisted of an indicative moisture trap (5 Å molecular sieves with dryerite, Activon, RDMT400D), a high-capacity coiled oxygen trap (Oxy-trap-large, Alltech, 4003), and an indicating oxygen trap (indicating Oxy-trap, Alltech, 4004). The flow was then regulated using a gas flowmeter (Cole Parmer, brass, standard valve, H 03294-00). Formal potentials were obtained from the midpoint of the anodic and cathodic peak currents ($E_f = (E_{pc} + E_{pa})/2$). The peak-to-peak separation (ΔE_p) was obtained from the difference (mV) between the anodic and cathodic peak currents ($\Delta E_p = E_{pc} - E_{pa}$).

X-ray Crystallography. A pale orange plate-like crystal was attached to a thin glass fiber and mounted on a Bruker SMART 1000 CCD diffractometer employing graphite monochromated Mo Kα radiation generated from a sealed tube. Cell constants were obtained from a least-squares refinement against 954 reflections located between 5.32 and 56.23° 2θ. Data were collected at $T =$ 294(2) K with ω scans to 56.60° 2θ. The intensities of 155 standard reflections recollected at the end of the experiment did not change significantly during data collection. Data integration and reduction were undertaken with SAINT and XPREP,[31] and subsequent computations were carried out with the *teXsan*[32] graphical user interface. A Gaussian absorption correction and an empirical correction determined from SADABS were applied to the data.[31] Data reduction also included the application of Lorentz and polarization corrections. The structure was solved and assigned to the space group $P\bar{1}$ (No. 2) by direct methods with *SIR97*[33] and extended and refined with *SHELXL-97*.[34] Anisotropic thermal parameters were refined for the non-hydrogen model atoms, and a riding-atom model was used for hydrogen atoms. Details of the crystallographic data for **3** are presented in Table 1.

Results

Complexes **1**−**3**, ruthenium(II) complexes of ligands **L1**−**L3**, respectively, were prepared by treatment of each ligand with a solution of tricarbonyldichlororuthenium(II) dimer in THF for 18 h, according to the literature procedure[30] for the preparation of the corresponding complex of 6,6′-dimethyl-2,2′-bipyridine (ligand **L4**). Complex **4**, Ru**L4**$(CO)_2Cl_2$, was also prepared as a reference compound. Tricarbonyldichlororuthenium(II) dimer was also used to provide coordinated

(31) Bruker *SMART*, *SAINT*, *SADABS*, and *XPREP* area detector control and data integration, reduction, and correction software; Bruker Analytical Intsruments Inc.: Madison, WI, 1995.
(32) *teXsan* for Windows (single-crystal structure analysis software); Molecular Structure Corporation: The Woodlands, 1997−1998.
(33) Altomare, A.; Cascarano, M.; Giacovazzo, C.; Guagliardi, A. *J. Appl. Crystallogr.* **1993**, *26*, 343.
(34) Sheldrick, G. M. *SHELX97: Program for Crystal Structure Refinement*; University of Gottingen, 1997.

Table 1. Crystallographic Data for **3**

empirical formula	$C_{16}H_{12}Cl_2N_2O_6Ru$
formula wt	500.25 g/mol
temperature	21 °C
space group	$P\bar{1}$ (No. 2)
a	8.917(2) Å
b	13.569(3) Å
c	7.827(2) Å
α	93.780(4)°
β	100.158(4)°
γ	100.539(4)°
V	911.6(4) Å^3
D_c	1.822 g cm^{-3}
Z	2
λ (Mo Kα)	0.71073 Å
μ (Mo Kα)	1.189 mm^{-1}
residuals[a] R1(*F*), wR2(F^2)	0.0203, 0.0544

[a] $R1 = \Sigma||F_o| - |F_c||/\Sigma|F_o|$ for $F_o > 2\sigma(F_o)$; $wR2 = (\Sigma w(F_o^2 - F_c^2)^2/\Sigma(wF_c^2)^2)^{1/2}$ for all reflections; $w = 1/[\sigma^2(F_o^2) + (0.0303P)^2 + 0.2564P]$ where $P = (F_o^2 + 2F_c^2)/3$.

carbonyls to the resulting metal complexes as coligands that are detectable by ^{13}C NMR spectroscopy; hence, these ligands may provide information on the stereochemistry and coordination geometry of the complexes. The complexes were isolated by filtration and characterized by microanalysis, IR spectroscopy, and ^1H NMR spectroscopy and by ^{13}C and ^{15}N NMR spectroscopy using heteronuclear single quantum coherence (HSQC) and heteronuclear multiple bond coherence (HMBC) techniques. ^{15}N NMR spectroscopy has been shown to be a useful probe for the determination of the site(s) of coordination of transition metal ions in ligands containing multiple potential binding sites, and it typically gives large chemical shift changes.[35−41] While the low abundance of ^{15}N makes this nuclei particularly insensitive to NMR detection, inverse detection methods allowed data on ligands **L1**−**L4** and complexes **1**−**4** to be obtained. The experiments were optimized to detect coupling to H3 of ring B (ligands **L1** and **L2**) and to H3,3′ in ligands **L3** and **L4** (<2 Hz). ^{13}C NMR spectroscopy was also used to characterize the complexes; in particular, it was used to determine whether the carbonyl groups were coordinated to the metal because this binding mode has been proposed for streptonigrin (Figure 1). In the case of complex **3**, single crystals suitable for X-ray diffraction analysis were obtained. Complex **2** was also studied using cyclic voltammetry to determine the influence of the metal on the redox potential of the quinone.

Complex 1. Treatment of **L1** with tricarbonyldichlororuthenium(II) dimer afforded [Ru(**L1**−CH_3)$(CO)_3$Cl] **(1)** (Scheme 1). Demethylation of the methoxyl group in **L1** was evident from the ^1H NMR spectrum of the complex and from

Scheme 1

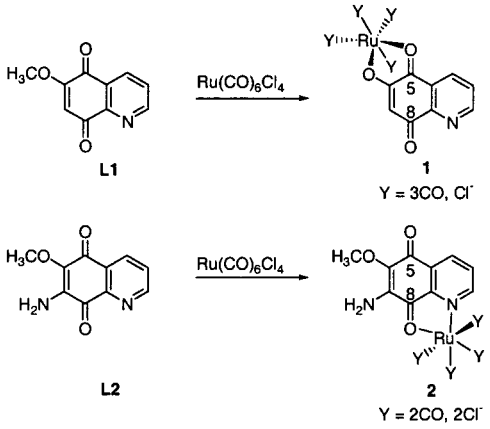

Table 2. ^{15}N Chemical Shifts in ppm (40.5 MHz, acetone-d_6) for Ligands **L1**−**L4** and Complexes **1**−**4**

compound	pyridyl N	NH_2
L1	315	
1	330	
L2	314	62
2	258	60
L3	307	
3	231, 247	
L4	307	
4	255	

microanalytical data, which also confirmed the presence of one chloro and three carbonyl ligands coordinated to the metal.

Complexation of ruthenium to the quinone and to the deprotonated hydroxyl oxygens rather than to the pyridyl nitrogen was confirmed by ^{15}N NMR data (Table 2). Compared to the ^{15}N signal of **L1**, a small downfield shift (15 ppm) of the ^{15}N signal was observed. This change is much less than those reported for other metal complexes involving a heterocyclic nitrogen[35] or for the changes observed for complexes **2** and **3** (see Table 2) in which direct coordination of ruthenium to the pyridyl nitrogen resulted in a change in the ^{15}N chemical shift of 50−60 ppm. While ^{13}C spectra were also recorded to ascertain the influence of the metal on the chemical shift of the carbonyl carbon (C5), complex **1** was not sufficiently soluble to allow detection of the quaternary carbons in a reasonable amount of time (i.e., <5 days).

Complex 2. Treatment of **L2** with tricarbonyldichlororuthenium(II) dimer under identical conditions to those used to prepare complex **1** (Scheme 1) afforded [Ru**L2**$(CO)_2Cl_2$] (**2**) in which the pyridyl nitrogen and adjacent quinoline oxygen are coordinated to the metal. The presence of the amino substituent alters the electron distribution in ring A, and demethylation of the adjacent methoxyl group did not occur. There are several potential binding sites in ligand **L2**, including the amino nitrogen and adjacent quinone oxygen. The small change in the ^{15}N chemical shift of the amino nitrogen (2 ppm) compared to the large upfield shift of the pyridyl nitrogen (−56 ppm) confirmed the coordination of the metal to the pyridyl nitrogen (Figure 2, Table 2). The ^{13}C chemical shift of adjacent quinone carbon (C8) was also shifted downfield by 9.6 ppm, which is consistent with the

(35) Satake, A.; Koshino, H.; Nakata, T. *J. Organomet. Chem.* **2000**, *595*, 208.
(36) Juranic, N.; Vuk-Pavlovic, S.; Nikolic, A. T.; Chen, T. B.; Macura, S. *J. Inorg. Biochem.* **1996**, *62*, 117.
(37) Juranic, N.; Macura, S. *Inorg. Chim. Acta* **1994**, *217*, 213.
(38) Schenetti, L.; Mucci, A.; Longato, B. *J. Chem. Soc., Dalton Trans.* **1996**, *3*, 299.
(39) van Stein, G. V.; van Koten, G.; Vrieze, K.; Brevard, C.; Spek, A. L. *J. Am. Chem. Soc.* **1984**, *106*, 4486.
(40) Buchanan, G. W.; Stothers, J. B. *Can. J. Chem.* **1982**, *60*, 787.
(41) Pregosin, P. S.; Streit, H.; Venanzi, L. M. *Inorg. Chim. Acta* **1980**, *38*, 237.

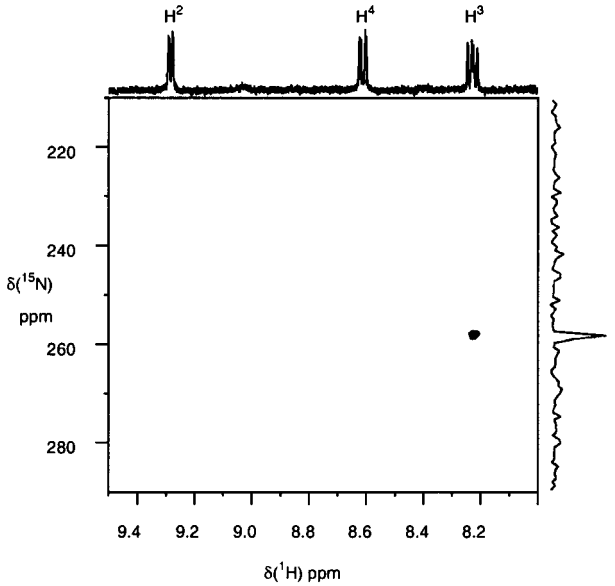

Figure 2. ^{15}N correlation spectrum of complex **2** (acetone-d_6, 40 MHz).

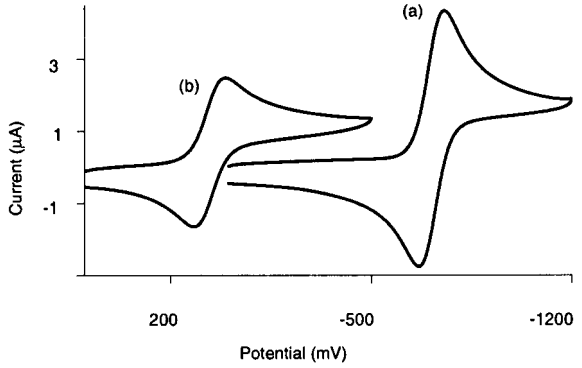

Figure 3. Cyclic voltammogram of (a) ligand **L1** and (b) complex **1** in THF. Scan rate = 100 mV s^{-1}, T = 295 K.

coordination of the quinone oxygen to the metal. Satisfactory elemental analysis could not be obtained for **2**, and signals due to residual THF were present in the ^{1}H NMR spectrum of **2** after it was dried under vacuum for 7 days. However, the mass spectrum gave the expected isotope pattern for the presence of one ruthenium and one chlorine atom, and the higher-mass peak was further characterized by measurement of a high-resolution mass spectrum. The presence of bound carbonyl ligands was confirmed by infrared spectroscopy, and sequential loss of these ligands and the chlorines was observed in the fragmentation pattern of the mass spectrum. Despite numerous attempts, crystals suitable for X-ray diffraction, which would define the stereochemistry of the coordinated chloro and carbonyl ligands in **2**, were not obtained.

The redox potential of the quinolinedione in **2** was measured in THF with TBAP as the electrolyte and was referenced to a Ag/AgCl reference electrode. The formal potential was shifted from −711 mV (ΔE_p = 87 mV) for **L2** to +64 mV (ΔE_p = 107 mV) for the ruthenium complex **2** (Figure 3). The Ru(II)/Ru(III) peaks were not observed.

Complex 3. Treatment of **L3** with tricarbonyldichloro-ruthenium(II) dimer yielded orange single crystals of

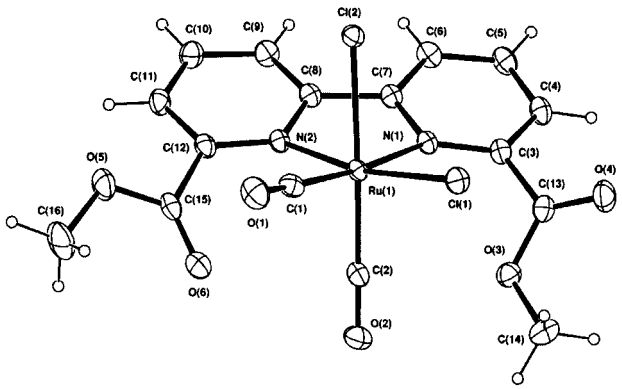

Figure 4. ORTEP depiction and numbering scheme for complex **3**, with atomic displacement ellipsoids shown at the 25% level.

Table 3. Selected Bond Lengths (Å) for **3**

Ru(1)−C(2)	1.880(2)	Ru(1)−C(1)	1.914(2)
Ru(1)−N(2)	2.1167(14)	Ru(1)−N(1)	2.1567(14)
Ru(1)−Cl(1)	2.3886(7)	Ru(1)−Cl(2)	2.4417(8)
O(1)−C(1)	1.076(2)	O(2)−C(2)	1.126(2)

Table 4. Selected Bond Angles (deg) for **3**

C(2)−Ru(1)−C(1)	89.89(8)	N(1)−Ru(1)−Cl(1)	94.49(4)
C(2)−Ru(1)−N(2)	96.91(7)	C(2)−Ru(1)−Cl(2)	176.53(6)
C(1)−Ru(1)−N(2)	98.95(7)	C(1)−Ru(1)−Cl(2)	86.68(6)
C(2)−Ru(1)−N(1)	94.78(7)	N(2)−Ru(1)−Cl(2)	84.17(4)
C(1)−Ru(1)−N(1)	174.62(7)	N(1)−Ru(1)−Cl(2)	88.67(4)
N(2)−Ru(1)−N(1)	77.87(6)	Cl(1)−Ru(1)−Cl(2)	87.299(17)
C(2)−Ru(1)−Cl(1)	92.05(6)	O(1)−C(1)−Ru(1)	178.41(19)
C(1)−Ru(1)−Cl(1)	87.99(6)	O(2)−C(2)−Ru(1)	176.12(18)
N(2)−Ru(1)−Cl(1)	168.65(4)		

[Ru**L3**$(CO)_2Cl_2$] (**3**) that were suitable for X-ray diffraction analysis. The coodination sphere geometry is summarized in Tables 3 and 4, and the numbering scheme is illustrated with an ORTEP[42,43] depiction in Figure 4. The octahedral metal coordination sphere in **3** is unremarkable. There are currently 23 dichoro-dicarbonyl-bipyridyl ruthenium-complex ligands listed on the CSD,[44] with mean ruthenium-to-chloride, rutheniun-to-carbonyl carbon, and ruthenium-to-bipyridyl nitrogen distances of 2.427, 1.892, and 2.097 Å, respectively. The mean carbonyl carbon-to-oxygen distance in the 23 CSD complexes is 1.122 Å.

The bipyridyl ligand least-squares plane in **3** is inclined 30° with respect to the equatorial least-squares plane of the complex, thus reducing the contact between the bipyridyl ester groups and the equatorial chloro and carbonyl ligands. The O3 ester functional group's least-squares plane forms a dihedral angle of 39° with the bipyridyl plane, and the ester group is rotated with respect to the bipyridyl plane such that O4 is pointed away from the chloro ligand and O3 is pointed toward the slightly electropositive C2 of the axial carbonyl dipole. The O5 ester residue forms a least-squares plane dihedral angle of 29° with the bipyridyl plane, and O6 is orientated toward the partially electropositive carbonyl carbons C1 and C2.

(42) Hall, S. R.; duBoulay, D. J.; Olthof-Hazekamp, R. *Xtal3.6* system; University of Western Australia: Perth, 1999.
(43) Johnson, C. K. *ORTEP II*; Report ORNL-5138; Oak Ridge National Laboratory: Oak Ridge, TN, 1976.
(44) Allen, F. H.; Kennard, O. *Chem. Des. Autum. News* **1993**, *8*, 31.

The coordination asymmetry in the solid state was also evident in the ^{1}H, ^{13}C, and ^{15}N NMR spectra of complex **3**. The ^{15}N NMR spectrum of **3** gave the expected upfield shifts of −60 and −76 ppm upon complexation of the two pyridyl nitrogens (Table 1). The upfield signal (δ 231 ppm) was assigned to the pyridyl nitrogen that is trans to the carbonyl ligand (see Figure 4). In addition to the bound-ligand peaks, the coordinated carbonyls were detected in the ^{13}C spectrum at 192.3 and 196.8 ppm, around 30 ppm downfield from the two ester side-chain carbonyl groups. Strong absorptions at 2013 and 2017 cm^{-1} also confirmed the presence of the bound carbonyl ligands.

Discussion

Streptonigrin contains many potential coordination sites including the 2,2-bipyridyl group, the picolinic acid system, the 2,2′-bipyridyl system, the aminoquinone system, the 2-(3′-amino-2′-pyridyl)quinoline system, and the amino and phenolic groups on rings C and D. Characterization of metal complexes of streptonigrin has been difficult to carry out because of the presence of multiple binding sites, the difficulty in crystallizing mixtures of complexes, the use of labile metals, and the limited structural information that is available from ^{1}H NMR spectroscopy because of the presence of only two aromatic hydrogens on the pyridyl rings.

The three ruthenium complexes **1**−**3** represent stable metal complexes of the AB and BC subunits that are present in the antitumor antibiotic streptonigrin. Standard ^{1}H and ^{13}C{^{1}H} spectra of these simple complexes were accompanied by HSQC and HMBC experiments to unambiguously establish the structures of the complexes and to collect ^{13}C and ^{15}N chemical shift data that could be used as structural probes to identify metal binding sites in the complex molecule streptonigrin in solution.

L1 and **L2** differ from each other only by one amino substituent but form significantly different coordination complexes. **L1** underwent a demethylation reaction in the presence of ruthenium, and chelation to the adjacent two oxygen ligands occurred in preference to chelation to the pyridyl nitrogen−quinone oxygen site (i.e., a different binding mode from the one that has been proposed to exist in streptonigrin) (Figure 1). Analogous aromatic demethylations in the presence of ruthenium have been reported. For example, tris coordination between tetracarboxylatodiruthenium(II,III) chloride and di(*o*-methoxyphenyl)formamidinate is reported, with dinitrogen chelation of the ruthenium accompanied by demethylation of the *o*-methoxyether and subsequent phenoxy coordination.[45] Addition of base to a ruthenium sandwich-type complex has also been reported to result in cleavage of a phenylmethyl ether.[46] A corresponding demethylation did not occur with **L2**, and the presence of the amino group directs the coordination in favor of the pyridyl site. Hence, in the design of metal complexes of streptonigrin, the substitution pattern of ring A is important, and removal of the amino group from this ring may lead to formation of different metal complexes, particularly with ruthenium(II).

^{15}N NMR has been used as an effective NMR probe to monitor metal complexation in a number of different systems.[35−41] Table 2 summarizes the key ^{15}N NMR data for complexes **1**−**3** and complex **4**[30] formed with 6,6′-dimethyl-2,2′-bipyridine **L4**. Given the difficulty in crystallization of metal complexes of streptonigrin, the ^{15}N data provides an informative diagnostic probe for monitoring metal binding to the pyridyl versus amino nitrogens in solution. While most studies support the formation of bipyridyl-type complexes of streptonigrin (Figure 1), complexes involving coordination to the amino substituent on ring B have been proposed,[4,17] and in the presence of an excess amount of the metal ion,[13,19] metal binding to the amino and oxygen atoms as well as to the 2,2′-bipyridyl group in streptonigrin cannot be ruled out.

The large upfield ^{15}N shift of the pyridyl nitrogens in complexes **3** and **4** was attributed to the coordination of the the nitrogens to ruthenium(II) in solution and is consistent with the coordination observed in the crystal structures of **3** and **4**.[30] An X-ray structure of **2** could not be obtained; however, the 56 ppm upfield shift of the pyridyl nitrogen of **2** provides direct evidence for the structure of **2**, which could not be unambiguously confirmed solely on the basis of ^{1}H and ^{13}C NMR spectroscopic data.

^{13}C NMR data were also measured to determine whether the quinone oxygen(s) were involved in the coordination sphere. This information is important because the electron density on ring A has a direct impact on the redox potential of the quinone and hence on the generation of radical species. This situation is illustrated in the effect the ruthenium coordination has on the redox potential of the quinolinedione in complex **2** (Figure 3), in which a quasi-reversible one-electron process is observed. Both the reduction and subsequent reoxidation of the quinolinedione shifted to a more positive value of the potential, indicating that ruthenium(II) complexation facilitates the production of radical species in THF. Independent studies of the effects of a variety of transition metal ions on the redox potential of streptonigrin and ligands **L1** and **L2** in aqueous solutions show similar trends.[47]

Ligand **L3** contains the key metal binding site in streptonigrin. The ester groups were incorporated to mimic the carbonyl groups in the quinone (ring A) and carboxylic acid (ring C) functions. The corresponding diacid was not used because of very poor solubility that makes purification difficult. Our previous studies on model ligands[48−50] have shown that the amino group on ring C is not involved in metal coordination, and hence this substituent was omitted from the ligand design. The crystal structure of **3** shows that,

(45) Ren, T.; DeSilva, V.; Zou, G.; Lin, C.; Daniels, L. M.; Campana, C. F.; Alvarez, J. C. *Inorg. Chem. Commun.* **1999**, *2*, 301.
(46) Kimura, M.; Morita, M.; Mitani, H.; Okamoto, H.; Satake, K.; Morosawa, S. *Bull. Chem. Soc. Jpn.* **1992**, *65*, 2557.
(47) Anderberg, P. I.; Harding, M. M.; Lay, P. A. In preparation.
(48) Long, G. V.; Boyd, S. E.; Harding, M. M.; Buys, I. E.; Hambley, T. W. *J. Chem. Soc., Dalton Trans.* **1993**, 3175.
(49) Long, G. V.; Harding, M. M.; Xie, M. C. L.; Buys, I. E.; Hambley, T. *J. Chem. Soc., Dalton Trans.* **1995**, *6*, 951.
(50) Long, G. V.; Harding, M. M.; Turner, P. *Polyhedron* **2000**, *19*, 1067.

despite the hindered 2,2′-bipyridyl binding site, formation of an octahedral 1:1 ligand/metal complex is possible. We have also recently reported a six-coordinate zinc(II) complex of a related ligand containing an amino group on the C ring.[50] In this zinc(II) complex, in contrast to **3**, the ester carbonyl groups coordinate to the metal to complete an octahedral coordination sphere that includes two axial water molecules.

The CSD currently lists only three 6,6′ disubstituted 2,2′-bipyridyl ruthenium complexes: dichloro-dicarbonyl(6,6′-dimethyl-2,2′-bipyridine)ruthenium(II),[30] hydrido-isothiocyanato-dicarbonyl-(6,6′-dimethyl-2,2′-bipyridine)ruthenium-(II),[30] and dichloro-(6,6′-bis(4-(*S*)-isopropyl-oxazolin-2-yl)-2,2′-bipyridine)ruthenium(II).[51] The bipyridyl planes of the first two complexes are inclined with respect to the equatorial coordination plane to reduce equatorial ligand contact in the same manner as that found in **3**. In contrast, the equatorial ligand plane and the plane defined by the equatorial coordination atoms in the isopropyloxazolinylbipyridyl complex are essentially coplanar. The oxazolinyl nitrogen atoms coordinate to the ruthenium from much the same position as the ester carbonyl oxygens of **3** might otherwise coordinate to the metal center, as seen in an analogous zinc complex.[50]

(51) Nishiyama, H.; Park, S.; Haga, M.; Aoki, K.; Itoh, K. *Chem. Lett.* **1994**, 1111.

In conclusion, the formation of complexes **1**−**3** suggests that streptonigrin will form stable, redox-active 1:1 bipyridyl complexes with ruthenium(II) or other metals favoring octahedral coordination. Metal coordination alters the charge distribution across the molecule (see Figure 1) and affects the redox potential of the quinone and hence directly influences the rate of generation of DNA-damaging radical species. Metal coordination also influences the conformational flexibility of the drug, which may have significant consequences in vivo. Studies of the synthesis and biological properties of these and related metal complexes that are based on the streptonigrin skeleton are currently under investigation in our laboratory.

Acknowledgment. This research was supported in part by the Sydney University Cancer Research Fund (M.M.H.). P.I.A. acknowledges receipt of an Australian Postgraduate Award.

Supporting Information Available: X-ray crystallographic files in CIF format for the structure determination of **3**. This information is available free of charge via the Internet at http://pubs.acs.org.

IC010876M